IEEE Access
Multidisciplinary | Rapid Review | Open Access Journal

Received March 7, 2018, accepted April 3, 2018, date of publication April 9, 2018, date of current version June 29, 2018.

Digital Object Identifier 10.1109/ACCESS.2018.2824334

Load-Isolation Wireless Power Transfer With K-Inverter for Multiple-Receiver Applications

JIWEI KUANG, BIN LUO, YANLING ZHANG, YAO HU, AND YIQIANG WU
School of Information Engineering, Nanchang University, Nanchang 330031, China

Corresponding author: Bin Luo (bil32@pitt.edu)

This work was supported in part by the National Natural Science Foundation of China under Grant 61461031, in part by the Natural Science Foundation of Jiangxi, China, under Grant 20161BAB202044, and in part by the China Scholarship Council under Grant 201706825057.

ABSTRACT Disturbances among the receivers caused by irrelevant circuit topology and inductive cross couplings among the receiving coils are particularly problematic aspects of multi-receiver wireless power transfer (WPT) systems. This paper proposes an effective and convenient scheme in which a K-inverter is inserted between an approximately 0 Ω output impedance voltage source and a transmitting resonator in order to isolate the receivers from each other, where the voltage and power distributed to each load are independent of other loads. The load-isolation principle is illustrated in detail. The indirect cross coupling aggravating the cross interferences is also investigated, and some practical criterions are derived to eliminate them. A three-receiver WPT experimental platform was established and tested to verify the theory; measured results were in close agreement with the theoretical values.

INDEX TERMS Wireless power transfer, multi-receiver, cross coupling, K-inverter, load-isolation.

I. INTRODUCTION

Resonant wireless power transfer (WPT) has garnered a great deal of research interest due to its mid-range transfer, tidiness, safe, and high efficiency [1]. The potential to wirelessly power multiple electronic devices (e.g., mobile phones and laptops) simultaneously via one transmitting coil is a particularly interesting concept [2].

There have been many studies to date on the multi-receiver (RX) WPT system. The feasibility of powering several receivers simultaneously was first established by Kurs *et al.* [3]. Frequency tracking [4], [5] and optional resonant frequencies [6], [7] were later proposed to improve the transmission efficiency for multi-RX WPT applications. Impedance matching techniques [2], [8]–[10] can also be utilized to deliver the transferred power to multiple receivers in a certain power division ratio. Load-independent output voltage analysis of multi-receiver WPT system has been proposed [30]. In [31], it has been shown that frequency configuration and distribution design of receivers can make the receivers get stable power for WPT systems with single relay and multi-receiver.

A typical multi-RX WPT system [11], [12] consists of one transmitter (TX) and multiple receivers (RXs) where the TX is driven by an AC voltage source denoted by the amplitude V_S and angular frequency ω_0, as shown in Fig. 1; the loss resistances brought about by the source, the capacitors, and the inductances are neglected for simplicity.

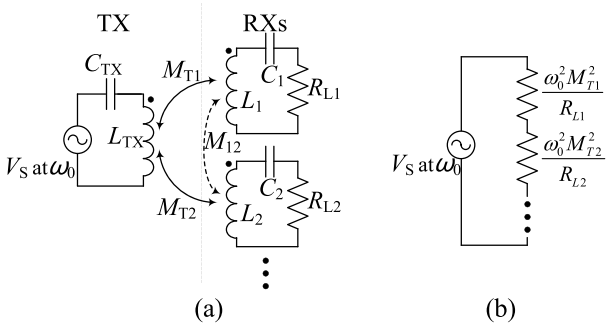

FIGURE 1. (a) Schematic diagram of conventional multi-RX WPT system; (b) equivalent circuit at the operating frequency neglecting cross couplings (e.g.,M_{12}).

The electric power is transferred from TX to RXs via magnetic resonance couplings among the TX and RX windings and delivered to each RX according to load impedances R_{Li} ($i = 1, 2, 3, \ldots$) and mutual inductances such as M_{T1} and M_{T2}. A crucial issue that does not exist in single RX WPT applications is that the power delivered to each RX may be significantly impacted by the others: For example, the voltage and the power delivered to RX1 are determined not only by

the circuit parameters (R_{L1}, M_{T1}, and V_S) of the TX and RX1, but also by the other RXs as shown in Fig. 1(b). The irrelevant circuit topology for multi-RX WPT (Fig. 1(a)) causes the voltage and power delivered to each RX to shift dramatically if an incoming RX is brought into (or a fully-recharged RX is removed from) the system. The multiple power path effects [13], [14] caused by the mutual inductances between the RX windings also mean that RX1 not only draws energy via the direct path of TX-RX1, but via other indirect routes (e.g., TX-RX2-RX1) as well as other RXs. Thus, multi-path power transfer can aggravate the cross interferences among RXs.

The cross interferences among RXs have two main sources. RXs are still disturbed, however, when mutual inductances between the RX windings are ignored [15]. A load-isolation scheme is crucial for managing the irrelevant circuit topology for multi-RX WPT systems.

In a realistic multi-RX WPT system – and especially in cases where a number of small appliances must be powered simultaneously – it is necessary that when a fully-recharged RX is removed from or a new RX is joined to the system randomly, all other RXs that are wirelessly charging remain unaffected; the voltage and the power on each RX should remain stable regardless. It is a fundamental requirement, but not a thoroughly researched objective, in multi-RX WPT systems that all RXs obtain the appropriate voltage and power from the power supply under the maximum energy efficiency principle [16] while staying isolated from other RXs during the charging period.

In this study, an effective and handy WPT structure for multi-RX WPT applications was established by inserting a K-inverter between the voltage source V_S and the series LC transmitting resonator composed of C_{TX} and L_{TX}. The K-inverter [19], also known as the impedance inverter, has been widely utilized in previous WPT studies [9], [17], [18] as impedance matching and power division devices. The K-inverter can also be used to isolate RXs from each other, as discussed below. As shown in Fig. 2(b), all loads are equivalent to being connected in parallel with the voltage source in the proposed scheme; thus, the voltage and power distributed to each load are independent of other RXs and remain unchanged even if other RXs are moved into or removed from the system at random.

In Section II, the load-isolation principle is illustrated in detail under circuit theory and several applicable K-inverters (T-type, Π-type, inductance coupled resonance circuits) and the derived Source Resonator (SR)-TX-RXs structure is discussed in detail. Formulas for the transmission efficient, voltage, and power contributing to each load are provided. Section III describes our experimental wireless charging platform with the SR-TX-RXs structure and three RXs, which we built to take measurements to compare against the theoretical values. Conclusions and future research directions are discussed in Section IV.

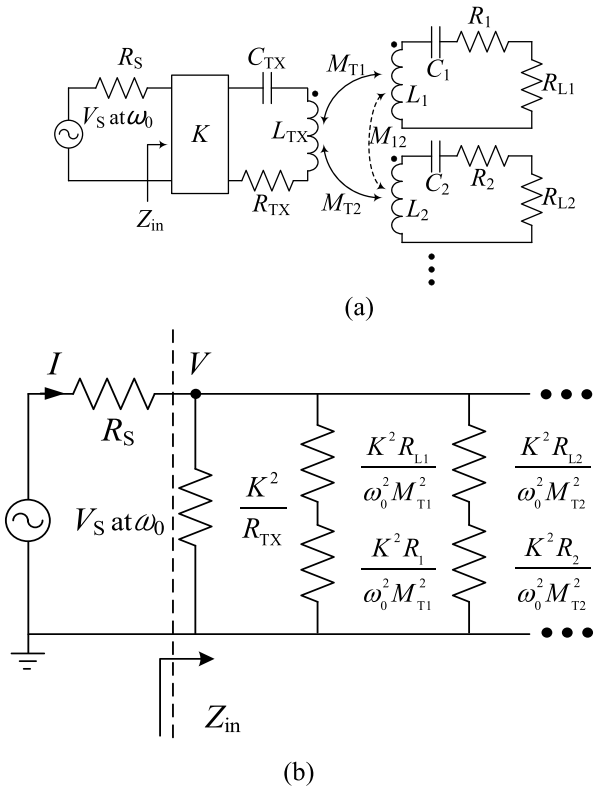

FIGURE 2. (a) Proposed WPT model; (b) equivalent circuit at the operating frequency.

II. CIRCUIT STRCTURE AND LOAD ISOLATION

A. PROPOSED CIRCUIT STRUCTURE

A schematic diagram of the proposed WPT model is shown in Fig. 2(a). The power supply V_S is composed of a half- or full-bridge converter driven by a DC power supply or an AC-DC circuit, which has a very little switching loss at the milliohm-scale and can be roughly treated as a constant voltage source with 0 Ω output impedance [9], [17]. Certain voltage sources (such as those composed of a high-frequency signal source or a linear power amplifier) have a remarkable output impedance in general – say, 50 Ω – and thus are not appropriate for the source in our model.

The other parameters include:

L_{TX}, L_i– the inductance of TX and RX-i respectively, with $i = 1, 2, 3, \ldots, N$, where N denotes the number of receivers;

C_{TX}, C_i– compensation capacitors;

R_{TX}, R_i– loss resistance in the inductances and capacitors;

M_{Ti}– mutual inductance between TX and the i- th RX;

M_{ij}– mutual inductance between the i-th and$j$-th RXs, where i or $j = 1, 2, 3, \ldots, N$ and $i \neq j$;

R_{Li}– resistive load of RX-i.

Although the inductive or capacitive load may shift the resonant frequency from the original one, it can always be compensated by an LC network [11]–[13] and thus is generally described as an equivalent resistance for simplicity.

All resonators are tuned at the same operating angular frequency ω_0, i.e.:

$$\omega_0 = 1/\sqrt{L_{TX}C_{TX}} = 1/\sqrt{L_1C_1} = 1/\sqrt{L_2C_2} = \ldots \quad (1)$$

The K-inverter inserted between the power supply and the transmitter resonator is a two-port device. Its ABCD matrix [19] can be expressed as follows

$$[A] = \pm\begin{pmatrix} 0 & \mathrm{j}K \\ \mathrm{j}/K & 0 \end{pmatrix} \quad (2)$$

where K is the characteristic parameter measured in Ohm. It can be implemented by a two-port lumped T-type or Π-type LC circuit [9] as shown in Fig. 3(a) with

$$L = K/\omega_0; \quad C = 1/(\omega_0 K) \quad (3)$$

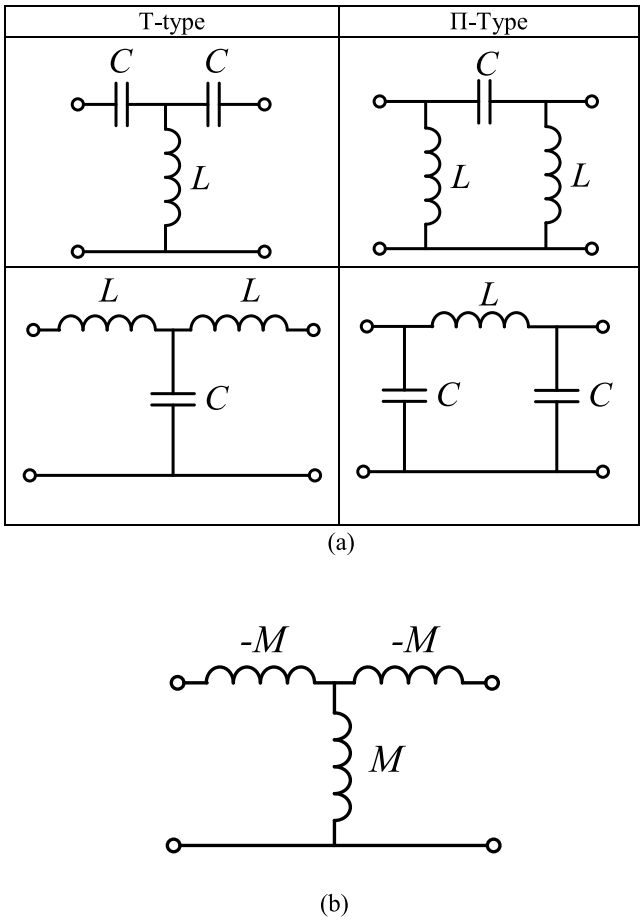

FIGURE 3. (a) Four lumped LC circuits; (b) inductance coupling circuit for K-inverter implementation.

or it can be realized by the inductance coupling circuit [17] in Fig. 3(b), where

$$M = K/\omega_0 \quad (4)$$

A variant SR-TX-RXs WPT can be derived by utilizing the inductance coupling circuit in Fig. 3(b) as the K-inverter. Compared with utilizing the lumped LC circuit in Fig. 3(a) as the K-inverter, utilizing the inductance coupling circuit is a better choice in this article because the K parameter can be adjusted conveniently per Eq. (4) by modifying the mutual inductance between the SR and TX coils to regulate the distance, transverse misalignment, or included angle between them in the proposed WPT system. However unwanted cross couplings $M_{Si}(i = 1, 2, 3, \ldots)$ between the source resonator winding and the RX windings need to be considered. As shown in Fig. 4(a), a series LC resonator resonating at ω_0 was inserted between the AC voltage

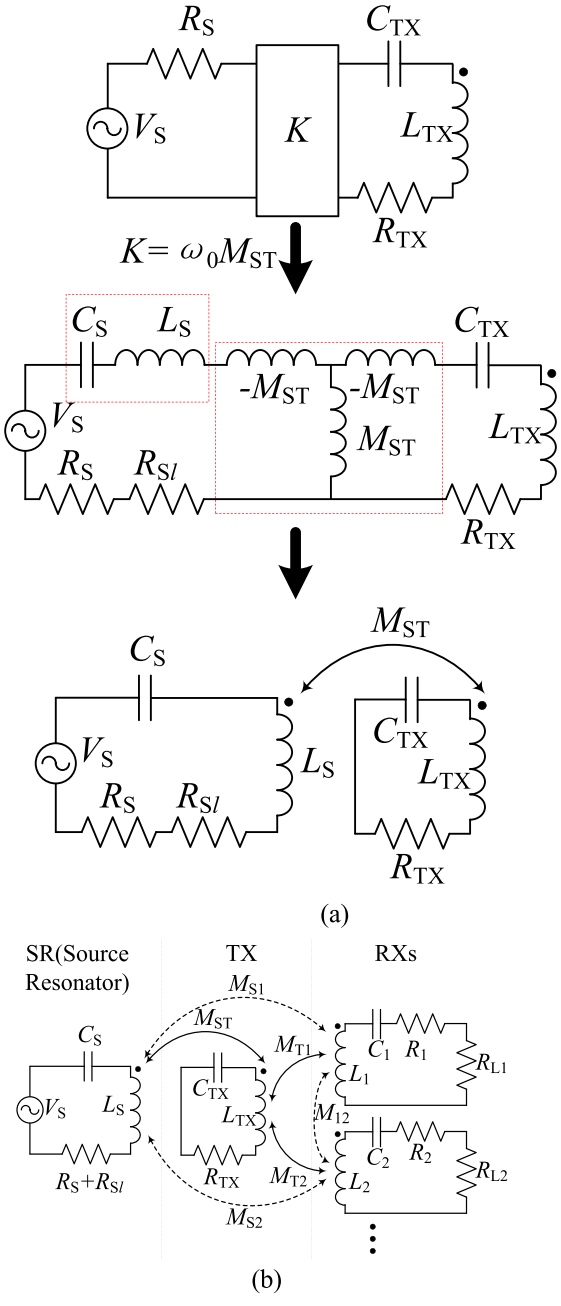

FIGURE 4. (a) Transformations converting the K-inverter to the inductance coupling circuit, where $R_{S/}$ indicates the loss of L_S; (b) schematic diagram of SR-TX-RXs WPT system, where M_{S1} , M_{S2}, etc. indicate mutual inductances due to cross couplings between L_S and receiving coils.

source and the K-inverter to compensate the minus mutual inductance, i.e., $-M_{ST}$, so that $L_S > M_{ST}$. The TX resonator constituted with L_{TX} and C_{TX} actually functions as a repeater or an intermediate resonator [13], [14], [17], [20]. R_{Sl} here in the SR represents the loss resistances of L_S and C_S.

B. LOAD ISOLATION PRINCIPLE

For the WPT system operating at ω_0, consider the input impedance Z_{in} at the load side and operating frequency shown in Fig. 2(a). By circuit analysis, it can be calculated as follows

$$Z_{\text{in}} = \frac{K^2}{R_{TX} + \sum_{i=1}^{N} \frac{\omega_0^2 M_{Ti}^2}{(R_i + R_{Li})}} \tag{5}$$

thus the circuit in Fig. 2(a) is equivalent to that in Fig. 2(b), where the mutual inductances M_{ij} $(i, j = 1, 2, 3 \ldots; i \neq j)$ can be set aside provisionally in order to conveniently analyze the function of the K-inverter. The phase information of the load voltages is totally lost during these transformations, but does not affect the system meaningfully– the voltage amplitudes and transferred powers are of concern and are both independent of the phases.

As shown in Fig. 2(a), the voltage V, across the load R_i and R_{Li} in i-th RX, is calculated by

$$V = V_s \frac{Z_{in}}{Z_{in} + R_s} \tag{6}$$

And the V_{Li} , the voltage of the R_{Li} in each RX, can be expressed as

$$\left(\frac{V}{K^2(R_{Li} + R_i)/\omega_0^2 M_{Ti}^2} \right)^2 \times \frac{K^2 R_{Li}}{\omega_0^2 M_{Ti}^2} = \frac{V_{Li}^2}{R_{Li}} \tag{7}$$

Due to (5), (6) and (7), the voltage amplitude of the load R_{Li} is derived as

$$|V_{Li}| = \frac{\omega_0 M_{Ti} V_S R_{Li}}{K(R_i + R_{Li})(1 + \frac{R_S R_{TX}}{K^2} + \sum_{i=1}^{N} \frac{\omega_0^2 M_{Ti}^2 R_S}{K^2(R_i + R_{Li})})} \tag{8}$$

To reduce the power dissipated during the power transmission from the source to RXs, the loss resistances R_S, R_{TX}, and R_i should be small enough to satisfy low-loss conditions. Generally, loss resistance R_i is far less than the load resistance R_{Li} and R_s is almost 0 Ω in the proposed WPT model. Thus

$$\frac{R_S R_{TX}}{K^2} \ll 1 \tag{9}$$

$$\frac{\omega_0^2 M_{Ti}^2 R_S}{K^2(R_i + R_{Li})} \ll 1 \tag{10}$$

$$R_i / R_{Li} \ll 1 \tag{11}$$

and

$$|V_{Li}| = \left| \frac{\omega_0 M_{Ti} V_S R_{Li}}{K(R_i + R_{Li})} \right| \approx \left| \frac{\omega_0 M_{Ti}}{K} \right| V_S \tag{12}$$

The power absorbed by R_{Li} can be determined as follows

$$P_{Li} \approx \frac{\omega_0^2 M_{Ti}^2 V_S^2 R_{Li}}{2K^2(R_i + R_{Li})^2} \approx \frac{\omega_0^2 M_{Ti}^2 V_S^2}{2K^2 R_{Li}} \tag{13}$$

Each load is equivalent to being connected in parallel with the AC power supply per the voltage transformation factor $|\omega_0 M_{Ti}/K|$. The voltage amplitude $|V_{Li}|$ is effectually determined by $|\omega_0 M_{Ti}/K|$ and V_S, i.e., it is independent of other RXs. As a result, moving any receiver in or out of the effective charging area of the WPT system does not affect the voltage or absorbed power of other loads. In short, all the loads are isolated from one another.

Further, the power absorbed by R_{Li} is mainly determined by the source voltage amplitude $|V_S|$, transformation factor $|\omega_0 M_{Ti}/K|$, and load of the i-th RX. For the applications of fixed power division ratios among the loads, the power received by RX-i can be adjusted flexibly by [altering the value of M_{Ti} in addition to modifying R_{Li} via impedance matching networks [2], [8], [21] without affecting the other loads.

Transmission efficiency is generally defined as the ratio of the transferred power to the available power [14], [20], [22]. So its value at ω_0 can be estimated as follows (Fig. 2(a))

$$\begin{aligned} \eta &= 2 \sum_{i-1}^{N} P_{Li} / Re(V_S I^*) \\ &= \frac{\sum_{i=1}^{N} \frac{\omega_0^2 M_{Ti}^2 R_{Li}}{K^2(R_i + R_{Li})^2}}{(\sum_{i=1}^{N} \frac{\omega_0^2 M_{Ti}^2}{K^2(R_i + R_{Li})} + \frac{R_{TX}}{K^2})} \\ &= \frac{\sum_{i=1}^{N} \frac{\omega_0^2 M_{Ti}^2 R_{Li}}{(R_i + R_{Li})^2}}{(\sum_{i=1}^{N} \frac{\omega_0^2 M_{Ti}^2}{(R_i + R_{Li})} + R_{TX})} \end{aligned} \tag{14}$$

For the SR-TX-RXs structure, $K = \omega_0 M_{ST}$, so Eq. (9) becomes

$$\frac{(R_S + R_{Sl}) R_{TX}}{\omega_0^2 M_{ST}^2} \ll 1 \tag{15}$$

which reflects strong coupling conditions [23]; Eqs. (12) and (13) can be further simplified as follows

$$|V_{Li}| \approx \left| \frac{\omega_0 M_{Ti} V_S R_{Li}}{\omega_0 M_{ST}(R_i + R_{Li})} \right| \approx \left| \frac{M_{Ti}}{M_{ST}} \right| V_S = \left| \frac{\omega_0 M_{Ti}}{K} \right| V_S \tag{16}$$

$$P_{Li} \approx \frac{M_{Ti}^2 V_S^2 R_{Li}}{M_{ST}^2 (R_i + R_{Li})^2} \approx \frac{M_{Ti}^2 V_S^2}{2 M_{ST}^2 R_{Li}} \tag{17}$$

The transmission efficiency formula in Eq. (14) still holds.

C. IMPACT OF CROSS COUPLINGS

As discussed above, the inductive cross couplings (ICCs) such as M_{ij} (which are usually well below the direct mutual inductances M_{Ti}) are neglected to simplify the analysis.

In practice, ICCs result in multi-path transfer of wireless power and may actually impact the multi-receiver WPT [6], [14], [24].

Determining the precise impact of ICCs is technologically difficult due to the necessity for a high-order full-element matrix equation with a large number of resonators for multi-RX WPT systems. There are two basic cases that help us draw some simple but applicable criteria to suppress ICCs and preserve the load isolation. We used the SR-TX-RXs WPT model as one case, in which the cross couplings include M_{Si}, the mutual inductances between the source resonator and the RXs except M_{ij}.

We first considered the cross coupling between the SR and RX for the SR-TX-RXs system (Fig. 4(b)) with only one receiver. At the center frequency ω_0, the coupled circuit matrix equation can be written as follows

$$\begin{pmatrix} R_{\mathrm{S}}+R_{\mathrm{Sl}} & \mathrm{j}\omega_0 M_{\mathrm{ST}} & \mathrm{j}\omega_0 M_{\mathrm{S1}} \\ \mathrm{j}\omega_0 M_{\mathrm{ST}} & R_{\mathrm{TX}} & \mathrm{j}\omega_0 M_{\mathrm{T1}} \\ \mathrm{j}\omega_0 M_{\mathrm{S1}} & \mathrm{j}\omega_0 M_{\mathrm{T1}} & R_1+R_{\mathrm{L1}} \end{pmatrix} \begin{pmatrix} I_{\mathrm{S}} \\ I_{\mathrm{TX}} \\ I_1 \end{pmatrix} = \begin{pmatrix} V_{\mathrm{S}} \\ 0 \\ 0 \end{pmatrix} \tag{18}$$

By ignoring R_{S}, R_{Sl}, R_{TX}, and R_1 for simplicity, the complex voltage amplitude on R_{Li} is

$$V_{L1} = \frac{-\omega_0 M_{\mathrm{T1}} R_{\mathrm{L1}} V_{\mathrm{S}}}{-2\mathrm{j}\omega_0^2 M_{\mathrm{T1}} M_{\mathrm{S1}} + \omega_0 M_{\mathrm{ST}} R_{\mathrm{L1}}} \tag{19}$$

If $M_{\mathrm{S1}} = 0$, then (19) becomes

$$V_{L1} = -\frac{\omega_0 M_{\mathrm{T1}} R_{\mathrm{L1}} V_{\mathrm{S}}}{\omega_0 M_{\mathrm{ST}} R_{\mathrm{L1}}} = -\frac{M_{\mathrm{T1}} V_{\mathrm{S}}}{M_{\mathrm{ST}}} = -\frac{\omega_0 M_{Ti}}{K} V_{\mathrm{S}} \tag{20}$$

which is clearly consistent with Eq. (12). Comparison between Eqs. (20) and (19) suggests that the impact of M_{S1} on V_{L1} is negligible when

$$|\omega_0 M_{\mathrm{S1}}| \ll \left|\frac{M_{\mathrm{ST}}}{M_{\mathrm{T1}}}\right| R_{\mathrm{L1}} \tag{21}$$

Next, to investigate the cross coupling among the RXs, write the circuit equation of the WPT system with two loads as follows

$$\begin{pmatrix} R_{\mathrm{S}}+R_{\mathrm{Sl}} & \mathrm{j}\omega_0 M_{\mathrm{ST}} & \mathrm{j}\omega_0 M_{\mathrm{S1}} & \mathrm{j}\omega_0 M_{\mathrm{S2}} \\ \mathrm{j}\omega_0 M_{\mathrm{ST}} & R_{\mathrm{TX}} & \mathrm{j}\omega_0 M_{\mathrm{T1}} & \mathrm{j}\omega_0 M_{\mathrm{T2}} \\ \mathrm{j}\omega_0 M_{\mathrm{S1}} & \mathrm{j}\omega_0 M_{\mathrm{T1}} & R_1+R_{\mathrm{L1}} & \mathrm{j}\omega_0 M_{12} \\ \mathrm{j}\omega_0 M_{\mathrm{S2}} & \mathrm{j}\omega_0 M_{\mathrm{T2}} & \mathrm{j}\omega_0 M_{12} & R_2+R_{\mathrm{L2}} \end{pmatrix} \begin{pmatrix} I_{\mathrm{S}} \\ I_{\mathrm{TX}} \\ I_1 \\ I_2 \end{pmatrix} = \begin{pmatrix} V_{\mathrm{S}} \\ 0 \\ 0 \\ 0 \end{pmatrix} \tag{22}$$

where $R_{\mathrm{S}}+R_{\mathrm{Sl}}$, R_{TX}, R_1, and R_2 are the loss resistances in SR, TX, RX1, and RX2, respectively. By neglecting M_{S1}, M_{S2}, and these loss resistances for further simplification, the complex voltage amplitude on R_{L1} can be written as follows

$$V_{L1} = \frac{\mathrm{j}\omega_0 M_{\mathrm{T2}} M_{12} - M_{\mathrm{T1}} R_{\mathrm{L2}}}{\omega_0^2 M_{\mathrm{ST}} M_{12}^2 + M_{\mathrm{ST}} R_{\mathrm{L1}} R_{\mathrm{L2}}} R_{\mathrm{L1}} V_{\mathrm{S}} \tag{23}$$

To simplify the analysis, it can be expressed in another form

$$V_{L1} = \frac{j\omega_0 M_{12} - \frac{M_{T1}}{M_{T2}} R_{L2}}{M_{ST}(\omega_0^2 M_{12}^2 + R_{L1} R_{L2})} M_{T2} R_{L1} V_S \tag{24}$$

If $\mathrm{M}_{12} = 0$, Eq. (24) can be degenerated to Eq. (20).According to Eq. (24), the impact of M_{12} on V_{L1} can be totally ignored if

$$|\omega_0 M_{12}| \ll \min\left(\left|\frac{M_{T1}}{M_{T2}}\right| R_{L2}, \sqrt{R_{L1} R_{L2}}\right) \tag{25}$$

The expression of V_{L2} can also be obtained by simply swapping the subscript 1 with 2 in Eq. (23):

$$|\omega_0 M_{12}| \ll \min\left(\left|\frac{M_{T2}}{M_{T1}}\right| R_{L1}, \sqrt{R_{L1} R_{L2}}\right) \tag{26}$$

By extending Eqs. (21), (25), and (26) to the applications with N receivers, then

$$|\omega_0 M_{Si}| \ll \left|\frac{M_{ST}}{M_{Ti}}\right| R_{Li} \quad \text{for } 1 \le i \le N \tag{27}$$

$$|\omega_0 M_{ij}| \ll \min\left(\left|\frac{M_{Ti}}{M_{Tj}}\right| R_{Lj}, \left|\frac{M_{Tj}}{M_{Ti}}\right| R_{Li}, \sqrt{R_{Li} R_{Lj}}\right) \quad \text{for } 1 \le i, j \le N \text{ and } i \ne j \tag{28}$$

If Eqs. (27) and (28) are satisfied, the impact of M_{ij} and M_{si} on the proposed WPT system can be absolutely ignored, and thus

$$V_{Li} = -\frac{M_{Ti}}{M_{ST}} V_S = -\frac{\omega_0 M_{Ti}}{K} V_S \tag{29}$$

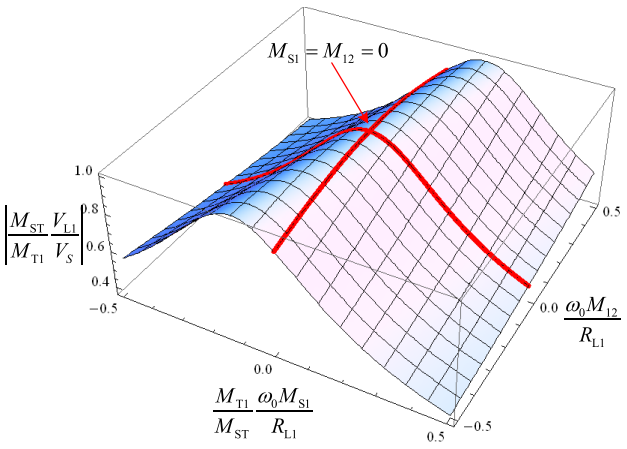

FIGURE 5. V_{L1} amplitude curve varies with M_{S1} and M_{12} under $M_{T1} = M_{T2}$, $M_{S1} = M_{S2}$, $R_{L1} = R_{L2}$; losses in the resonators are neglected.

An example of the V_{L1} amplitude curve varying with M_{S1} and M_{12} for a SR-TX-RXs WPT system with two RXs was calculated by Eq. (20) and plotted in Fig. 5 under the conditions $M_{\mathrm{T1}} = M_{\mathrm{T2}}$, $M_{\mathrm{S1}} = M_{\mathrm{S2}}$, and $R_{\mathrm{L1}} = R_{\mathrm{L2}}$ with the losses in the resonators ignored. Fig. 5 shows that reducing the valve of ω_0/R_{L1} and ω_0/R_{L2} leads to less disturbance by the cross couplingM_{S1}, M_{S2} and M_{12} on $|V_{\mathrm{L1}}|$

and $|V_{L2}|$. In other words, heavy resistive and low operating frequency, which make the valve of ω_0/R_{L1} and ω_0/R_{L2} smaller, can reduce the impact of the cross couplings while keeping the receivers and the source resonator far away from each other; and these conclusions also hold for multi-RX applications with lumped LC circuits as the K-inverters.

III. NUMERICAL SIMULATIONS AND EXPERIMENTS

In the SR-TX-RXs WPT system we propose, a large-caliber Helmholtz coil (Fig. 6) is chosen as the TX coil for experiment. A three-dimensional alternating uniform magnetic field can be produced inside the cylindrical space sketched by the Helmholtz coil [25] and excited by an AC source, thus the transmitting coil can guarantee that almost uniform power is delivered regardless of where a receiver is placed inside the coil. The large Helmholtz coil can not only keep the receivers and the' source resonator far away from each other so as to reduce M_{Si}, but also maintains suitable distances among receivers to depress M_{ij}. A schematic diagram of the experimental SR-TX-RXs WPT platform is shown in Fig. 7.

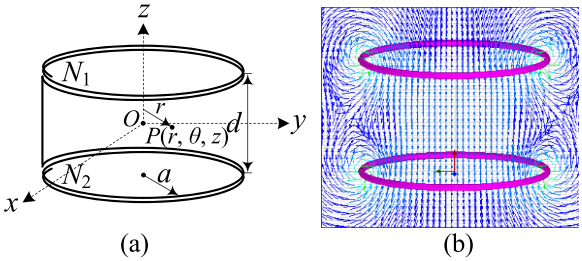

FIGURE 6. (a) Helmholtz coil and (b) surrounding simulated magnetic field structures.

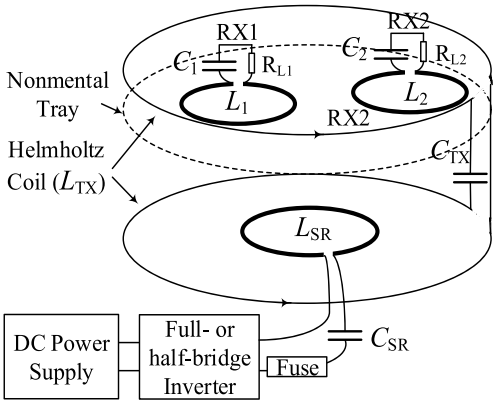

FIGURE 7. Schematic diagram of the proposed WPT system with large Helmholtz coil as the TX coil.

To verify the proposed theory (Section II), we built a SR-TX-RXs WPT experimental platform using a large circular two-layer Helmholtz coil as the TX coil as shown in Fig.8. Compared with Fig. 4(b), the platform chosen a coil instead of a lump inductor. As we know, with the same inductance, the Q of lump inductor usually is higher than that of the coil.

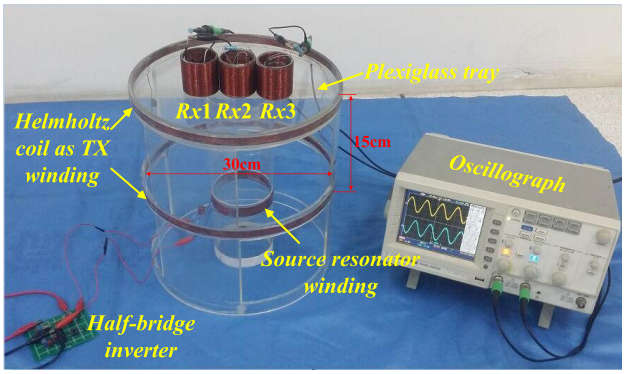

FIGURE 8. SR-TX-RXs experimental platform with Helmholtz coil as the TX winding.

In this experiment, the coil, which is convenient to replace to adjust the value of K, is just a component of the proposed WPT system. The AC voltage source was constructed with a half-bridge converter driven by a DC power supply with the DC output voltage set to 10 V; the peak voltage of the AC source V_S was approximately 6.36V [26].

For WPT applications, higher operating frequency (e.g., several MHz) is beneficial in increasing the Q factors of the resonators as well as the transmission efficiency. Slightly lower frequency (say, a few hundred KHz), however, can suppress the ICCs and allows for the inverter to be much more easily manufactured. Here, we set the operating frequency to 79.9 KHz.

Three receivers RX1, RX2, and RX3 connected in series with resistance of R_{L1}, R_{L2}, and R_{L3}, respectively, were placed closely adjacent to each other. The measured parameters of the resonators and mutual inductances in the experimental platform are listed in Table 1 and 2, where the loss resistance of SR includes R_S and R_{SI} (Fig. 4(b)).

TABLE 1. Resonator parameters in experimental platform.

	SR	TX	RX1&2&3
Number of turns	16	20	40
Wire diameter (mm)	1	1	1
Radius of coil (cm)	5	15	2.5
Inductance (μH)	42	186	60
Compensation capacitor (nF)	95	21	60
Loss resistance (Ω)	0.13	0.49	0.18

Fig. 9(a) shows the simulated and measured amplitude frequency curves of V_{L1}, V_{L2}, V_{L3}, and η under $R_{L1} = 10\Omega$ and $R_{L2} = R_{L3} = 5\Omega$. According to the experimental data in the Table 3, although each load value is different, almost the same voltage can be obtained for each load, and the cross-coupling between the loads does not cause much interference to the voltage obtained by the load. This also means that the K-inverter can effectively isolate the load. In this

TABLE 2. Mutual inductance among resonator coils.

Unit: μH	SR	RX1	RX2	RX3
SR	7.50	0.11	0.15	0.11
TX		4.37	4.38	4.38
RX1			3.01	0.58
RX2				3.02

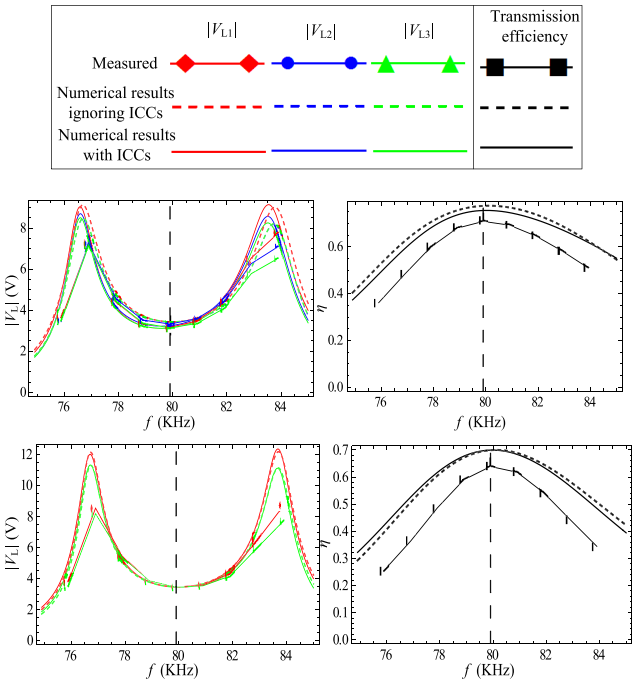

FIGURE 9. Measured voltage amplitudes on loads and transmission efficiency compared to numerical solutions. (a) Case 1: Three receivers coexist; (b) Case 2: RX2 removed from the platform.

TABLE 3. Measured, simulated and calculated results with three receivers.

Unit of voltage: V	V_{L1}	V_{L2}	V_{L3}	η
Measured results	3.28	3.08	3.22	72.8%
Simulated results (with ICCS)	3.47	3.27	3.41	74.1%
Simulated results (without ICCS)	3.60	3.54	3.54	79.0%
Calculated results (from the formulas)	3.64	3.58	3.58	80.9%

case, $|\omega_0 M_{12}| = |\omega_0 M_{23}| = 1.51\Omega$ almost reached one third of R_{L2}, so the measured peak voltages on the loads significantly deviated from the estimated values (up to 14%). In other words, ω_0/R_L was not small enough in these cases; suitable distance among the RXs must be kept to reduce the mutual inductance M_{ij}.

TABLE 4. Measured, simulated and calculated results with RX2 out.

Unit of voltage: V	V_{L1}	V_{L2}	V_{L3}	η
Measured results	3.55	0	3.49	64.8%
Simulated results (with ICCS)	3.60	0	3.54	70.8%
Simulated results (without ICCS)	3.60	0	3.54	70.9%
Calculated results (from the formulas)	3.64	0	3.58	72.0%

For further comparison, RX2 was removed from the charging zone to obtain the simulated and measured results shown in Fig. 9(b) and Table 4. In this case, RX2 was removed to keep the cross couplings small enough ($|\omega_0 M_{S1}| = |\omega_0 M_{S3}| = 0.055\Omega$ and $|\omega_0 M_{13}| = 0.291\Omega$) i.e., well below $R_{L1}(= 10\Omega)$ and $R_{L3}(= 5\Omega)$, so turbulence in the cross couplings could be entirely ignored. The measured peak voltage on the loads was in close agreement with the numerical and estimated (Eqs. (14) and (12)) results at 79.9 KHz.

Fig. 9 depicts the resonant frequency splitting phenomenon [16], [27]–[29], where the voltage amplitude-frequency curves indicate the operating frequency is located at the valley as opposed to the peaks on either side. The efficiency curves have a single peak with central peaks located at the operating frequency. It is crucial for most appliances to acquire the appropriate voltage and power rather than the maximum from the power supply to maximize efficiency – most mobile phones, for example, e.g., are charged with only 5 V DC voltage. Our scheme actually follows the maximum energy efficiency principle rather than the maximum power transfer principle [16].

To further investigate the load voltage amplitudes versus the loads, we fixed R_{L1} as 10Ω and adjusted R_{L3} from 5Ω to infinity after removing RX2; we measured and simulated the voltage amplitudes of V_{L1} and V_{L3} as plotted in Fig. 10, where $1/R_{L3}$ (rather than R_{L3}) was chosen as the abscissa to ensure R_{L3} approached infinity. In this case, RX3 was open-circuited or removed from the wireless charging zone. The results show that V_{L1} was almost unaffected by the load of RX3 and vice versa, even when RX3 was removed. In effect, when the cross couplings were well depressed, all receivers were well isolated from each other (Section II), so no impedance matching technologies were needed to dynamically adjust the load voltages when the receivers were added to or removed from the system. The load voltages also slightly decreased as R_{L3} was reduced.

As shown in Fig. 2(a), the current I_S and voltage on R_S increased as load resistance decreased, i.e., the voltages on the loads were less thoroughly distributed. If one RX in the charging area was short-circuited for some reason, a very large current would arise in the source and may damage the power source. Protective devices (e.g., a fuse) should be installed in the source resonator to prevent this.

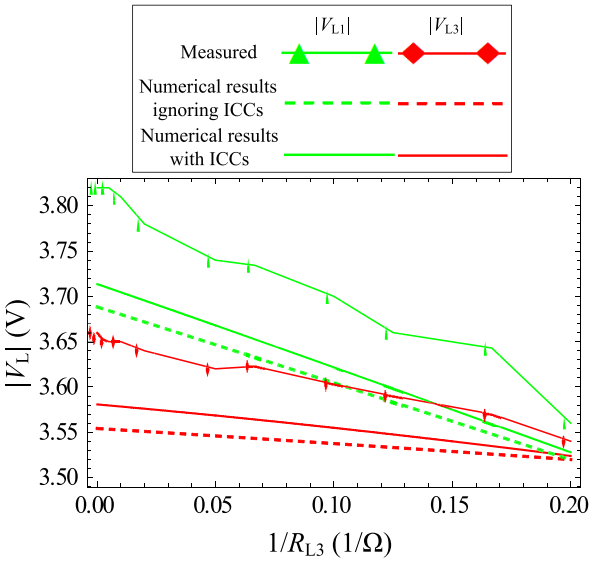

FIGURE 10. Measured and simulated voltage amplitudes on R_{L1} and R_{L3} vary with $1/R_{L3}$ when RX2 is removed.

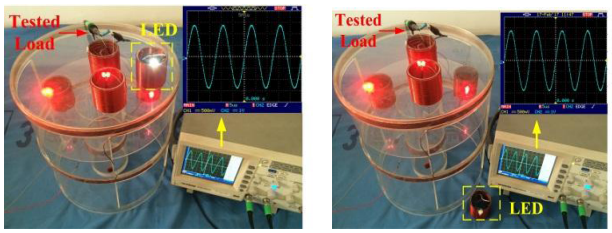

FIGURE 11. Load-isolation in the multi-RX WPT system: (a) Before and (b) after a high-power LED is joined in the system.

Fig. 11 shows where the voltage amplitudes across the tested load were almost the same before and after the high-power LED (dotted box) was moved in the system. This verifies the load-isolation feature of the proposed scheme.

FIGURE 12. An application of the SR-TX-RXs WPT system charging multiple LEDs and mobile phones.

Fig. 12 shows an example where several LEDs and mobile phones were powered wirelessly via the proposed scheme with a two-layer circular Helmholtz coil as the repeater winding.

IV. CONCLUSIONS

This paper proposed a novel scheme in which a K-inverter is utilized to achieve load-isolation in multi-RX WPT applications. The load-isolation principle was illustrated theoretically and verified by numerical simulations and experiments per key indexes such as the power contributing to each RX and the transmission efficiency.

The K-inverter can be implemented with an inductance coupling circuit in addition to a lumped T-type or Π-type LC circuit. In the inductance coupling circuit with a K-inverter, the SR-TX-RXs WPT topology is preferred because the K parameter can be adjusted conveniently.

By inserting a K-inverter between the half- or full-bridge AC voltage source and the TX in a traditional multi-RX WPT system, each receiver load is analogous to being connected in shunt with the power supply with approximately a 0 Ω output impedance. Each RX load absorbs the power from the power supply depending on the source voltage amplitude, the voltage transformation ratio $|\omega_0 M_{Ti}/K|$, and its own impedance; it is thus unaffected by any other receivers. The load-isolation feature is highly beneficial for charging many small appliances (e.g., mobile phones or laptops) simultaneously as they are added to or removed from the WPT system randomly and frequently.

We found that low operating frequency and heavy receiver loads are helpful in suppressing the cross couplings among the receiver coils and the SR coil. By configuring these parameters carefully, the effect of ICCs can be effectively managed.

The load-isolation concept introduced here may also be applicable in domino WPT [13], [14], [20] applications, which we plan to explore in our future research.

REFERENCES

[1] S. Y. R. Hui, W. Zhong, and C. K. Lee, "A critical review of recent progress in mid-range wireless power transfer," *IEEE Trans. Power Electron.*, vol. 29, no. 9, pp. 4500–4511, Sep. 2014.

[2] J. Kim, D.-H. Kim, and Y.-J. Park, "Analysis of capacitive impedance matching networks for simultaneous wireless power transfer to multiple devices," *IEEE Trans. Ind. Electron.*, vol. 62, no. 5, pp. 2807–2813, May 2015.

[3] A. Kurs, R. Moffatt, and M. Soljačić, "Simultaneous mid-range power transfer to multiple devices," *Appl. Phys. Lett.*, vol. 96, no. 4, p. 044102, 2010.

[4] B. L. Cannon, J. F. Hoburg, D. D. Stancil, and S. C. Goldstein, "Magnetic resonant coupling as a potential means for wireless power transfer to multiple small receivers," *IEEE Trans. Power Electron.*, vol. 24, no. 7, pp. 1819–1825, Jul. 2009.

[5] D. Ahn and S. Hong, "Effect of coupling between multiple transmitters or multiple receivers on wireless power transfer," *IEEE Trans. Ind. Electron.*, vol. 60, no. 7, pp. 2602–2613, Jul. 2013.

[6] W. Zhong and S. Y. R. Hui, "Auxiliary circuits for power flow control in multifrequency wireless power transfer systems with multiple receivers," *IEEE Trans. Power Electron.*, vol. 29, no. 9, pp. 5902–5910, Oct. 2015.

[7] Y. Zhang, T. Lu, Z. Zhao, F. He, K. Chen, and L. Yuan, "Selective wireless power transfer to multiple loads using receivers of different resonant frequencies," *IEEE Trans. Power Electron.*, vol. 30, no. 11, pp. 6001–6005, Nov. 2015.

[8] J. Kim, H.-C. Son, D.-H. Kim, and Y.-J. Park, "Impedance matching considering cross coupling for wireless power transfer to multiple receivers," in *Proc. IEEE Wireless Power Transf. (WPT)*, Perugia, Italy, May 2013, pp. 226–229.

[9] K. E. Koh, T. C. Beh, T. Imura, and Y. Hori, "Impedance matching and power division using impedance inverter for wireless power transfer via magnetic resonant coupling," *IEEE Trans. Ind. Appl.*, vol. 50, no. 3, pp. 2061–2070, May/Jun. 2014.
[10] K. Lee and D. H. Cho, "Analysis of wireless power transfer for adjustable power distribution among multiple receivers," *IEEE Antennas Wireless Propag. Lett.*, vol. 14, pp. 950–953, 2015.
[11] Y.-J. Kim, D. Ha, W. J. Chappell, and P. P. Irazoqui, "Selective wireless power transfer for smart power distribution in a miniature-sized multiple-receiver system," *IEEE Trans. Ind. Electron.*, vol. 63, no. 3, pp. 1853–1862, Mar. 2016.
[12] Y. Zhang, T. Lu, Z. Zhao, F. He, K. Chen, and L. Yuan, "Employing load coils for multiple loads of resonant wireless power transfer," *IEEE Trans. Power Electron.*, vol. 30, no. 11, pp. 6174–6181, Nov. 2015.
[13] W. X. Zhong, C. K. Lee, and S. Y. R. Hui, "Wireless power domino-resonator systems with noncoaxial axes and circular structures," *IEEE Trans. Power Electron.*, vol. 27, no. 11, pp. 4750–4762, Nov. 2012.
[14] C. K. Lee, W. X. Zhong, and S. Y. R. Hui, "Effects of magnetic coupling of nonadjacent resonators on wireless domino-resonator systems," *IEEE Trans. Power Electron.*, vol. 27, no. 4, pp. 1905–1916, Apr. 2012.
[15] J. J. Zhou, B. Luo, X. X. Zhang, and Y. Hu, "Extendible load-isolation wireless charging platform for multi-receiver applications," *IET Power Electron.*, vol. 10, no. 1, pp. 134–142, Jan. 2017.
[16] S. D. Barman, A. W. Reza, N. Kumar, M. E. Karim, and A. B. Munir, "Wireless powering by magnetic resonant coupling: Recent trends in wireless power transfer system and its applications," *Renew. Sustain. Energy Rev.*, vol. 51, pp. 1525–1552, Nov. 2015.
[17] B. Luo, S. Wu, and N. Zhou, "Flexible design method for multi-repeater wireless power transfer system based on coupled resonator bandpass filter model," *IEEE Trans. Circuits Syst. I, Reg. Papers*, vol. 61, no. 11, pp. 3288–3297, Nov. 2014.
[18] K. K. Ean, B. T. Chuan, T. Imura, and Y. Hori, "Novel band-pass filter model for multi-receiver wireless power transfer via magnetic resonance coupling and power division," in *Proc. Wireless Microw. Technol. Conf.*, Cocoa Beach, FL, USA, Apr. 2012, pp. 1–6.
[19] J. S. Hong and M. J. Lancaster, *Microstrip Filters for RF/Microwave Applications*. New York, NY, USA: Wiley, 2001, pp. 38–75.
[20] W. Zhong, C. K. Lee, and S. Y. R. Hui, "General analysis on the use of Tesla's resonators in domino forms for wireless power transfer," *IEEE Trans. Ind. Electron.*, vol. 60, no. 1, pp. 261–270, Jan. 2013.
[21] Y. Lim, H. Tang, S. Lim, and J. Park, "An adaptive impedance-matching network based on a novel capacitor matrix for wireless power transfer," *IEEE Trans. Power Electron.*, vol. 29, no. 8, pp. 4403–4413, Aug. 2014.
[22] I. Awai and T. Ishizaki, "Design of 'magnetic resonance type' WPT systems based on filter theory," *Electron. Commun. Jpn.*, vol. 96, no. 10, pp. 1–11, 2013.
[23] A. Karalis, J. D. Joannopoulos, and M. Soljačić, "Efficient wireless non-radiative mid-range energy transfer," *Ann. Phys.*, vol. 323, no. 1, pp. 34–48, 2008.
[24] M. Fu, T. Zhang, P. C.-K. Luk, X. Zhu, and C. Ma, "Compensation of cross coupling in multiple-receiver wireless power transfer systems," *IEEE Trans. Ind. Informat.*, vol. 12, no. 2, pp. 474–482, Apr. 2016.
[25] R. Beiranvand, "Analyzing the uniformity of the generated magnetic field by a practical one-dimensional Helmholtz coils system," *Rev. Sci. Instrum.*, vol. 84, no. 7, pp. 075109-1–075109-11, Jul. 2013.
[26] H. L. Li, A. P. Hu, G. A. Covic, and C. S. Tang, "Optimal coupling condition of IPT system for achieving maximum power transfer," *Electron. Lett.*, vol. 45, no. 1, pp. 76–77, Jan. 2009.
[27] A. P. Sample, D. T. Meyer, and J. R. Smith, "Analysis, experimental results, and range adaptation of magnetically coupled resonators for wireless power transfer," *IEEE Trans. Ind. Electron.*, vol. 58, no. 2, pp. 544–554, Feb. 2011.
[28] O. Karaca, F. Kappeler, D. Waldau, R. M. Kennel, and J. Rackles, "Eigenmode analysis of a multiresonant wireless energy transfer system," *IEEE Trans. Ind. Electron.*, vol. 61, no. 8, pp. 4134–4141, Aug. 2014.
[29] Y.-L. Lyu *et al.*, "A method of using nonidentical resonant coils for frequency splitting elimination in wireless power transfer," *IEEE Trans. Power Electron.*, vol. 30, no. 11, pp. 6097–6107, Nov. 2015.
[30] L. Sun, H. Tang, and S. Zhong, "Load-independent output voltage analysis of multiple-receiver wireless power transfer system," *IEEE Antennas Wireless Propag. Lett.*, vol. 15, pp. 1238–1241, 2016.
[31] W. Wang, X. Huang, J. Guo, H. Liu, C. Yan, and L. Tan, "Power stabilization based on efficiency optimization for WPT systems with single relay by frequency configuration and distribution design of receivers," *IEEE Trans. Power Electron.*, vol. 32, no. 9, pp. 7011–7024, Sep. 2017.

JIWEI KUANG received the B.E. degree from Nanchang University, China, in 2015, where he is currently pursuing the master's degree. His current research interests include the design and theory of antenna and wireless power transfer.

BIN LUO received the B.E. degree from the Department of Electronic Engineering and Information Science, University of Science and Technology of China, Hefei, in 1997, and the Ph.D. degree from the School of Information Science and Technology, University of Science and Technology of China, in 2005.

Since 2005, he has been serving as one of the faculty of the Department of Electronic Information Engineering, Nanchang University, Nanchang, China, where he is currently a Professor. He is currently a Visiting Scholar with the Swanson School of Engineering, University of Pittsburgh. His current research interests include the design and theory of antenna and wireless power transfer.

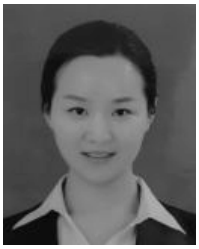

YANLING ZHANG received the B.E. degree from Henan Normal University, China, in 2016. She is currently pursuing the master's degree with Nanchang University, China. His current research interests include the design and theory of antenna and wireless power transfer.

YAO HU received the B.E. degree from the Hunan University of Arts and Science, China, in 2013. She is currently pursuing the master's degree with Nanchang University, China. Her current research interests include the design and theory of antenna and wireless power transfer.

YIQIANG WU received the B.E. degree from Nanchang University, China, in 1982. He currently serves as a Professor with the School of Information Engineering, Nanchang University. His current research interests include microwave and RF technology applications.